A&A 490, 769–776 (2008)
DOI: 10.1051/0004-6361:200809597

Astronomy & Astrophysics

Evolution and nucleosynthesis of extremely metal-poor and metal-free low- and intermediate-mass stars⋆

I. Stellar yield tables and the CEMPs

S. W. Campbell[1,2] and J. C. Lattanzio[2]

[1] Academia Sinica Institute of Astronomy and Astrophysics, PO Box 23-141, Taipei 10617, Taiwan
e-mail: simcam@asiaa.sinica.edu.tw
[2] Centre for Stellar and Planetary Astrophysics, School of Mathematical Sciences, Monash University, Melbourne 3800, Australia
e-mail: john.lattanzio@sci.monash.edu.au

Received 18 February 2008 / Accepted 23 August 2008

ABSTRACT

Context. The growing body of spectral observations of the extremely metal-poor (EMP) stars in the Galactic Halo provides constraints on theoretical studies of the chemical and stellar evolution of the early Universe.
Aims. To calculate yields for EMP stars for use in chemical evolution calculations and to test whether such models can account for some of the recent abundance observations of EMP stars, in particular the highly C-rich EMP (CEMP) halo stars.
Methods. We modify an existing 1D stellar structure code to include time-dependent mixing in a diffusion approximation. Using this code and a post-processing nucleosynthesis code we calculate the structural evolution and nucleosynthesis of a grid of models covering the metallicity range: $-6.5 \leq$ [Fe/H] ≤ -3.0 (plus $Z = 0$), and mass range: $0.85 \leq M \leq 3.0\ M_{\odot}$, amounting to 20 stars in total.
Results. Many of the models experience violent nuclear burning episodes not seen at higher metallicities. We refer to these events as "Dual Flashes" since they are characterised by nearly simultaneous peaks in both hydrogen and helium burning. These events have been reported by previous studies. Some of the material processed by the Dual Flashes is dredged up causing significant surface pollution with a distinct chemical composition. We have calculated the entire evolution of the $Z = 0$ and EMP models, from the ZAMS to the end of the TPAGB, including extensive nucleosynthesis. In this paper, the first of a series describing and analysing this large data set, we present the resulting stellar yields. Although subject to many uncertainties these are, as far as we are aware, the only yields currently available in this mass and metallicity range. We also analyse the yields in terms of C and N, comparing them to the observed CEMP abundances. At the lowest metallicities ([Fe/H] $\lesssim -4.0$) we find the yields to contain ∼1 to 2 dex too much carbon, in agreement with all previous studies. At higher metallicities ([Fe/H] ~ -3.0), where the observed data set is much larger, all our models produce yields with [C/Fe] values consistent with those observed in the most C-rich CEMPs. However it is only the low-mass models that undergo the Dual Shell Flash (which occurs at the start of the TPAGB) that can best reproduce the C *and* N observations. Normal Third Dredge-Up can not reproduce the observations because at these metallicities intermediate mass models ($M \gtrsim 2\ M_{\odot}$) suffer HBB which converts the C to N thus lowering [C/N] well below the observations, whilst if TDU *were* to occur in the low-mass ($M \leq 1\ M_{\odot}$) models (we do not find it to occur in our models), the yields would be expected to be C-rich only, which is at odds with the "dual pollution" of C and N generally observed in the CEMPs. Interestingly events similar to the EMP Dual Flashes have been proposed to explain objects similarly containing a dual pollution of C and N – the "Blue Hook" stars and the "Born Again AGB" stars. We also find that the proportion of CEMP stars should continue to increase at lower metallicities, based on the results that some of the low mass EMP models already have polluted surfaces by the HB phase, and that there are more C-producing evolutionary episodes at these metallicities. Finally we note that there is a need for multidimensional fluid dynamics calculations of the Dual Flash events, to ascertain whether the overproduction of C and N at ultra-low metallicities found by all studies is an artifact of the 1D treatment.

Key words. stars: evolution – stars: interiors – Galaxy: halo – stars: AGB and post-AGB

1. Introduction

In terms of chemical pollution the Extremely Metal Poor (EMP, [Fe/H] $\lesssim -2.5$) Galactic Halo stars are the most ancient objects currently known in the Universe. Observations show that their metallicities reach as low as [Fe/H] $= -5.5$ (Frebel et al. 2005) – far below the metallicities measured in damped Lyα systems for example. Studying the EMP stars is thus crucial to understanding the chemical evolution of the early Universe. They provide the best link we have to the elusive first generation of stars (Pop III). Indeed, the surface abundances of individual EMP stars are enriched to such a small degree that they may reflect the composition of the ejecta of only a few (or even one) Pop III supernovae. The chemical information from these stars should eventually aid in our understanding of the First Stars, providing indirect evidence for the chemical evolution of the Galaxy and, importantly, the first stellar mass function (FMF), which is still very uncertain. Deducing the FMF is also important in terms of the Epoch of Reionisation. For these reasons this field is often referred to as "Near Field Cosmology". The nearness of the EMP stars (relative to ancient objects at high redshift) also means that extremely detailed information can be collected from their spectra using current instruments.

⋆ Tables 1 to 6 are only available in electronic form at the CDS via anonymous ftp to cdsarc.u-strasbg.fr (130.79.128.5) or via http://cdsweb.u-strasbg.fr/cgi-bin/qcat?J/A+A/490/769

The discovery of Galactic Halo EMPs has naturally led to a renewed interest in the theoretical modelling of Population III and low-metallicity stars. In particular the subset of these ancient stars that is observed to contain large amounts of carbon, the C-rich EMPs (CEMPs, which we define here as stars with [C/Fe] $>$ +0.7, also see Fig. 5) has attracted much stellar modelling work since their abundance patterns are difficult to explain with standard stellar evolution. These interesting objects also appear to comprise a large proportion of the EMPs ($\sim$10 $\rightarrow$ 20%; see Beers & Christlieb 2005; Cohen et al. 2005; Lucatello et al. 2006), suggesting that an additional (or modified) source of C production was active in the early Universe. The CEMPs also display variation in a range of other elements, such as s-process species (e.g. Goswami et al. 2006; Aoki et al. 2006a; Sivarani et al. 2006; also see Beers & Christlieb 2005 for an overview of the observations). A number of theories have been proposed to explain the various abundance patterns seen in CEMPs, ranging from pre-formation pollution via Pop III supernovae (e.g. Shigeyama & Tsujimoto 1998; Limongi et al. 2003) to self-pollution through peculiar evolutionary events (e.g. Fujimoto et al. 2000; Weiss et al. 2004) to binary mass transfer (e.g. Suda et al. 2004).

In the current study we focus on the nature of the chemical pollution produced by low- and intermediate-mass (LM and IM) EMP and $Z = 0$ stars. As these stars generally don't produce the heavier elements (except possibly for s-process elements), we assume that they have formed from gas clouds already enriched by Pop III supernovae that produced the near scaled-solar abundances of many elements seen in the "normal" (non C-rich) EMP Halos stars. In terms of producing the excessive light element pollution evident in the CEMPs we keep an open mind as to whether they may have received their compositions through self-pollution events or through binary mass-transfer (be it from wind accretion or Roche lobe overflow).

Stellar modelling of low-mass EMP stars started in the early 1960s, when Ezer (1961) calculated ZAMS models of $Z = 0$ stars. In the early 1980s it was realised that low-mass EMP stars may suffer H-ingestion during the core He flash at the tip of the Red Giant Branch (D'Antona 1982). About ten years later this was confirmed by detailed simulations (Fujimoto et al. 1990; Hollowell et al. 1990). The H-ingestion during these evolutionary events – which are peculiar to models of low-mass $Z = 0$ and EMP stars – results in a rapid burning of the protons, a H-flash. More recent work has investigated the dependence of the H-ingestion flashes on physical inputs (e.g. Schlattl et al. 2001), compared the chemical signatures from the simulations with observations of CEMPs (e.g. Fujimoto et al. 2000; Chieffi et al. 2001) and explored the possibility of initiating the s-process at zero metallicity (Goriely & Siess 2001).

Although some grids of EMP and $Z = 0$ models have already been computed the studies have either ignored the H-ingestion events (e.g. Cassisi & Castellani 1993; Marigo et al. 2001) and/or have not calculated all of the AGB evolution. In the current study we aim to provide a homogeneous set of yields that include the nucleosynthetic effects of the EMP H-ingestion events (which we refer to below as "Dual Flashes"), AGB Third Dredge-Up (TDU, the periodic mixing up of He-burning products after a thermal pulse) and AGB Hot Bottom Burning (HBB, the H-burning of the convective envelope). To this end we have undertaken a broad exploration of EMP ($-6.5 \leq$ [Fe/H] ≤ -3.0) and $Z = 0$ stellar evolution and nucleosynthesis in the low and intermediate mass regime ($0.85 \leq M \leq 3.0\ M_{\odot}$). We include (for the first time) evolutionary and nucleosynthesis calculations from ZAMS to the end of the thermally-pulsing AGB phase (TPAGB) involving 74 species, as well as chemical yield tables. With this homogeneous set of models we hope to shed some light on whether or not 1D stellar models can help to explain some of the EMP halo star observations, and in particular the CEMP abundance patterns.

2. Method

Our simulations were performed utilising two numerical codes – a stellar structure code and post-processing nucleosynthesis code.

The stellar structure code used was the Monash version of the Monash/Mount Stromlo stellar evolution code (MONSTAR, see e.g. Wood & Zarro 1981; Frost & Lattanzio 1996). The code is largely a standard 1D code that utilises the Henyey-matrix method (a modified Newton-Raphson method) for solving the stellar structure equations. For the present study the instantaneous convective mixing routine was replaced by a time-dependent (diffusive) mixing routine (similar to that described by Meynet et al. 2004). This change was necessary due to the violent evolutionary events (the H-flashes) that occur in models of $Z = 0$ and EMP stars, where the timescale for mixing becomes comparable to the evolutionary time steps. Our numerical scheme remained the same, "partially simultaneous", which means mixing and structure are calculated within each iteration (see Stancliffe 2006 for a comparison of different methods).

Opacities have been updated to those from Iglesias & Rogers (1996) (for mid-range temperatures) and Ferguson et al. (2005) (for low temperatures). Convective boundaries were always defined by the Schwarzschild criterion – i.e. the search for a neutral convective boundary (see Frost & Lattanzio 1996) was not performed and no overshoot was applied.

A key problem with modelling EMP stars is the unknown driver(s) of mass loss. We have used the empirical mass-loss formula of Reimers (1975) during the RGB. We believe this to be acceptable because the mass lost prior to the AGB is very small due to the short-lived giant branches at these metallicities (see e.g. D'Antona 1982). For the AGB we use the formula of Vassiliadis & Wood (1993). As described below, all the models experience some self-pollution – and always before or at the very beginning of the TPAGB phase. We find that the surfaces of the AGB models usually have metallicities approaching that of the LMC or even Solar (as defined by $Z = 1 - X - Y$ rather than Fe – they are still Fe-poor). Thus, since the stellar surfaces have (some of) the ingredients needed to form grains, we argue that using a standard mass loss formula is warranted, at least as a first approximation. We note that metallicity is also indirectly taken into account by the mass loss formulae, since they depend on bulk stellar properties (such as radius, luminosity, pulsation period), which vary significantly with metallicity.

The nucleosynthesis calculations were made with the Monash Stellar Nucleosynthesis code (MONSOON), a post-processing code which takes input from the MONSTAR code (e.g. density, temperature, convective velocities). It solves a network of 506 nuclear reactions involving 74 nuclear species (see e.g. Cannon 1993; Lattanzio et al. 1996; Lugaro et al. 2004). The yield tables contain a reduced number of species because we have excluded isotopes with very short lifetimes (and thus have negligible yields).

Initial composition for the $Z = 0$ models was taken from the Standard Big Bang nucleosynthesis calculations of Coc et al. (2004), whilst the initial composition for the EMP models was derived by mixing the ejecta from a 20 $M_{\odot}$ $Z = 0$ supernova calculation (Limongi 2002, private communication) with varying

amounts of Big Bang material from Coc et al. (2004) to reach the desired [Fe/H] values (for example $10^6\,M_\odot$ of Big Bang material was required for [Fe/H] = −4.0). The main difference between this composition and that of a scaled-solar composition is an underabundance of N, since the supernova calculation did not produce much of this element. This was found to have little effect however since whenever the CNO cycle operates it quickly converts much of the C to N anyway ([C/Fe] is ∼0 initially).

Our grid of models covers the mass range: M = 0.85, 1.0, 2.0, 3.0 $M_\odot$ and the metallicity range: [Fe/H] = −6.5, −5.45, −4.0, −3.0, plus $Z = 0$.

3. Results and discussion

3.1. The dual flash events

As mentioned above it has long been known that theoretical models of $Z = 0$ stars (and EMP stars) undergo violent evolutionary episodes not seen at higher metallicities.

The most severe of these evolutionary events occurs during the core He flash of low-mass stars (with [Fe/H] $\lesssim -4.5$, see Fujimoto et al. 2000). In this event the normal flash-driven convection zone breaks out of the He-rich core. Thus H-rich material is mixed down to regions of high temperature, producing a secondary flash: a H-flash. This flash reaches luminosities comparable to the core He flash itself and exists concurrently with the He flash. Thus we refer to the combination of these events as a "Dual Core Flash" (DCF). These events have been given rather cumbersome names in the literature to date: e.g. Helium Flash Induced Mixing (HEFM, Schlattl et al. 2002) and Helium Flash-Driven Deep Mixing (He-FDDM, Suda et al. 2004). We propose the simpler name DCF to illustrate the essential nature of the phenomenon.

A similar event occurs in stellar models of higher mass and higher (although still very low) metallicities. In these cases it is the normal flash-driven convection zone present during the first pulse (or first few pulses) of the TPAGB phase that breach the H-He discontinuities. Again a H-flash results, concomitant with the He shell flash, so we refer to this event as a "Dual *Shell* Flash" (DSF). Cassisi et al. (1996) appear to be the first to have reported the occurrence of a DSF, although they were unable to follow the evolution of the event. DSFs have since been reported and modelled by a number of groups (e.g. Chieffi et al. 2001; Siess et al. 2002; Iwamoto et al. 2004).

Both the DCF and DSF events are driven by the same phenomenon: ingestion of protons into a hot region caused by expansions of He convective zones into H-rich regions. Thus our proposed nomenclature unifies them as being "Dual Flashes" and then distinguishes them again by referring to the driving event: be it the core or shell flash. Furthermore, the term only applies to H-flash events occurring at low metallicities.

Both the DCF and DSF have consequences for the surface composition of the star since, in both cases, the convective envelope subsequently deepens and mixes up the (processed) material overlying the H-burning shell. In Fig. 1 we display an example DCF event (our 1 $M_\odot$, [Fe/H] = −6.5 model). Here we can see the normal Helium-Flash Convective Zone (HeCZ) rapidly expanding into the H-rich regions above. The result is that a second convective zone, which is H-rich (HCZ) is set up by the rapid proton burning at its base (the H-flash). The HeCZ reduces in mass due to a reduction in He burning and, in this case, the two convective zones remain separated. A few thousand years later the convective envelope moves in and dredges up most of the processed material located above the H-exhausted core

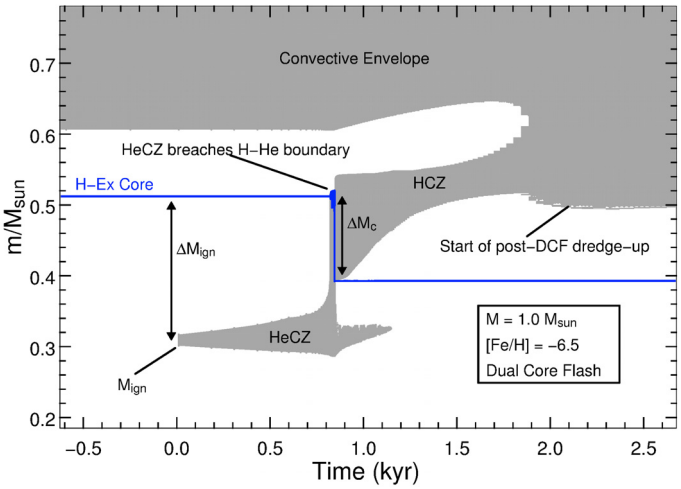

Fig. 1. Example of one of the Dual Core Flash events. Convective regions are shown by grey shading whilst the mass location of the edge of the H-exhausted core is shown by the solid line (blue).

(labelled H-Ex Core in the figure; only the beginning of this dredge-up is shown), causing a strong pollution of the stellar envelope. Since this model experiences no Third Dredge-Up during the AGB phase the DCF dredge-up is the main contributor to the chemical yield.

Interestingly the Dual Flash phenomenon (and subsequent dredge-up) is similar to the "Late Hot Flasher" scenario proposed to explain Blue Hook stars in Galactic globular clusters, where white dwarves produced from RGB stars with excessive mass loss experience a late core He-flash that engulfs the remaining H-rich envelope (see e.g. Sweigart 1997; Brown et al. 2001; Cassisi et al. 2003). Another similar phenomenon is the "Born Again" scenario for producing H-deficient post-AGB (PAGB) stars (such as Sakurai's Object; see e.g. Asplund et al. 1997). In this case a star that has recently left the AGB experiences a very late helium-shell flash that also engulfs the remaining H-rich envelope, again producing a H-flash (see e.g. Iben et al. 1983; Renzini 1990; Herwig et al. 1999). Both these scenarios lead to surface pollution similar to that produced by the DF events since the matter mixed up in these cases has also undergone H and He burning. We note however that the envelope mass overlying the He convective zones is much lower in both these cases ($\sim 10^{-4}\,M_\odot$) than in the EMP/$Z = 0$ Dual Flash case ($\sim 10^{-1}\,M_\odot$ or higher).

We discuss the chemical composition of the surface pollution resulting from the Dual Flash events when we compare the C and N yields with observations below (Sect. 3.3).

3.2. Nucleosynthetic yields and their categorisation

In Table 1 we present a sample of the yields for the models. A total of five tables with the same format as these are available in their entirety online at the CDS (Tables 1 to 5). Each table contains yields for models with initial stellar masses of 0.85, 1.0, 2.0 and 3.0 $M_\odot$ at each of the metallicities: [Fe/H] = −6.5, −5.45, −4.0, −3.0, and $Z = 0$. We list the yields for all the stable species used in the nucleosynthesis calculations, which range from ^{1}H to ^{34}S plus a small iron group (Ni, Co, Fe isotopes). We also provide yields for the important radionuclides ^{26}Al (which decays to ^{26}Mg) and ^{60}Fe (which decays to ^{60}Ni). Yields are given in mass fraction of each species in the total ejecta. In the tables we also give the initial compositions for each metallicity. The final masses (remnant core masses) are given in

Table 1. Part of the yield table for the $Z = 0$ models – selected species only. Initial composition is included in the third column.

Nuclide	A	Initial	0.85 $M_\odot$	1.0 $M_\odot$	2.0 $M_\odot$	3.0 $M_\odot$
^{1}H	1	7.548E–01	7.014E–01	6.597E–01	6.596E–01	5.807E–01
^{4}He	4	2.450E–01	2.976E–01	3.295E–01	3.367E–01	4.066E–01
^{7}Li	7	3.130E–10	4.704E–10	1.263E–09	4.491E–10	4.887E–11
^{12}C	12	0.000E+00	2.598E–05	1.844E–03	1.309E–04	4.882E–04
^{13}C	13	0.000E+00	7.778E–06	3.619E–04	3.034E–05	1.152E–04
^{14}N	14	0.000E+00	2.437E–04	3.919E–03	3.432E–03	1.166E–02
^{16}O	16	0.000E+00	5.034E–04	4.333E–03	4.885E–05	1.516E–04
^{19}F	19	0.000E+00	1.848E–09	6.225E–06	2.879E–10	1.188E–09
^{20}Ne	20	0.000E+00	2.485E–07	1.726E–06	2.737E–05	1.386E–04
^{23}Na	23	0.000E+00	1.291E–09	1.131E–05	1.294E–05	9.539E–05
^{24}Mg	24	0.000E+00	3.838E–11	1.362E–06	1.865E–07	2.630E–07
^{25}Mg	25	0.000E+00	1.459E–08	3.166E–07	1.756E–06	1.562E–05
^{26}Mg	26	0.000E+00	2.475E–08	4.065E–08	8.159E–06	6.889E–05
^{26}Al	26	0.000E+00	3.182E–11	3.364E–10	3.085E–07	1.487E–06
^{28}Si	28	0.000E+00	1.002E–07	1.649E–11	6.170E–07	1.315E–06
^{31}P	31	0.000E+00	2.200E–08	2.071E–12	5.219E–07	1.117E–06
^{32}32	32	0.000E+00	4.381E–09	1.224E–12	1.870E–07	2.665E–07

Table 6 (only at CDS). Using this information it is easy to convert the yields to any format. The yields are calculated by integrating the mass of each species lost by the star over its lifetime (τ_*):

$$M_i^{\rm tot} = \int_0^{\tau_*} X_i(t)\frac{{\rm d}M}{{\rm d}t}{\rm d}t \qquad (1)$$

where X_i is the mass fraction of species i. The total mass of each species lost to the ISM, $M_i^{\rm tot}$, is then scaled with $M_{\rm ej}$, the total mass lost by the star, to give the mass fractions.

In some cases our models failed to converge towards the end of the AGB. This is a common problem with stellar codes. Often there was very little mass left in the envelope so this was just added to the yields. However in some cases there was enough mass left that it would not have been lost in one interpulse period. In these cases we performed a short synthetic evolution calculation for the remaining thermal pulses (including third dredge-up and core growth) to complete the evolution, following the method of Karakas (2003). Yields were then calculated taking into account this extra mass loss. In most models the number of thermal pulses calculated in this way was $\lesssim$8. This represents between ∼1 and 10% of the total number of thermal pulses in most of our models. Thus the synthetic pulses generally have a minor impact on the yields.

As an example of the nucleosynthesis we show in Fig. 2 the results for our $M = 3\ M_\odot$ and [Fe/H] $= -5.45$ model. Here it is TDU and Hot Bottom Burning that are the main contributors to the yield of the star. Indeed, the chemical signature arising from the DSF occurring at the start of the AGB is totally erased by these normal AGB evolutionary episodes. In particular the CN cycling product ^{14}N dominates the surface composition during most of the AGB (in terms of metallic species). The ^{12}C/^{13}C and C/N ratios quickly approach equilibrium values once the (strong) HBB starts.

We summarise the self-pollution episodes over the whole grid of models by dividing them into three categories, defined by the evolutionary events/phases that dominate the chemical signature in the yields:

- Group 1 yields are dominated by the DCF events.
- Group 2 are dominated by DSF events.
- Group 3 are dominated by TDU+HBB.

Members of the DCF group have polluted surfaces during the horizontal branch phase onwards whilst the members of the DSF group have polluted surfaces after the first few pulses of the AGB (see Fig. 3). In the low mass models ($M \leq 1.0\ M_\odot$) this pollution occurs despite the lack of TDU. Thus our models predict a greater proportion of C-rich stars at extremely low metallicity, since these Dual Flash events do not occur at higher metallicities.

In Fig. 4 we show the self-pollution groups in a mass-metallicity diagram. Here it is clear that the yields of all the intermediate mass models ($M \geq 2.0\ M_\odot$) that suffer surface pollution resulting from Dual Shell Flashes are actually dominated by the pollution occurring during the AGB phase. In other words the

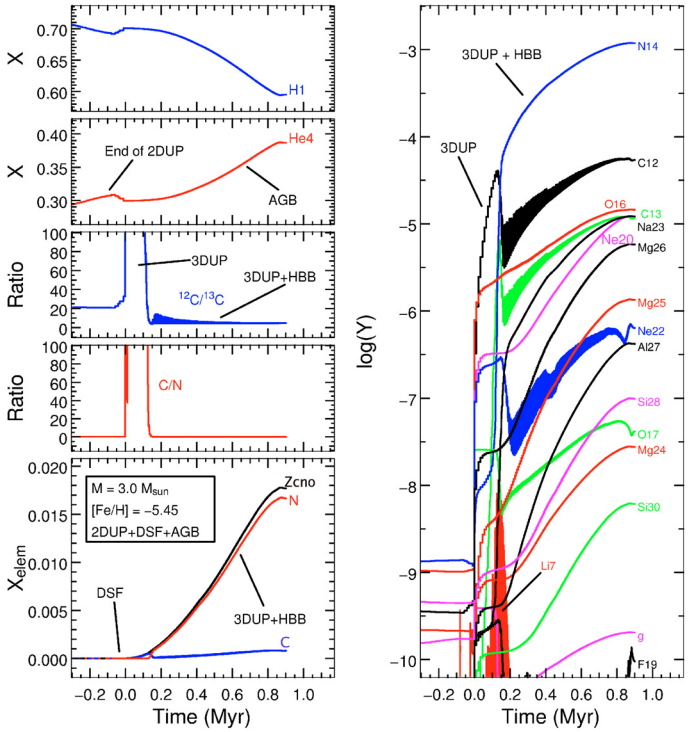

Fig. 2. Time evolution of the surface composition in the [Fe/H] $= -5.45$, 3 $M_\odot$ model, for selected species. This model is a member of our self-pollution Group 3 (see text and Fig. 3 for details). The rich nucleosynthesis arising from TDU and HBB is seen in the right-hand panel. This chemical signature by far dominates that of the DSF in this case (see *bottom left panel*).

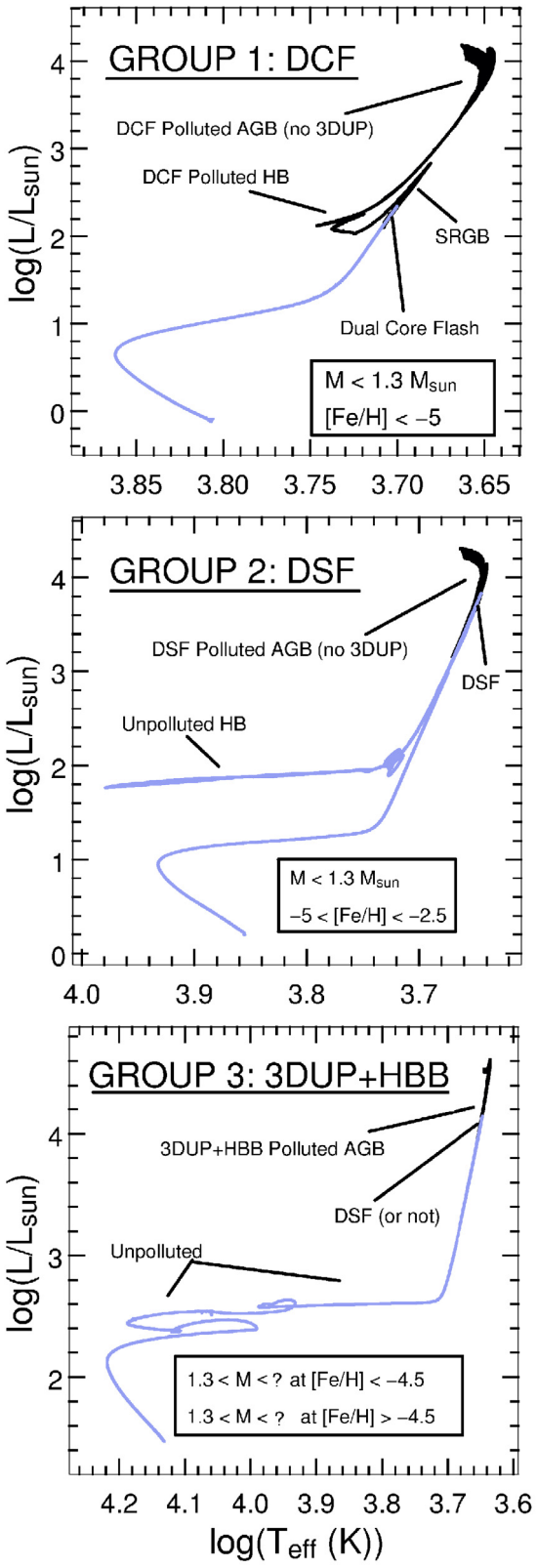

Fig. 3. Displayed in each HR diagram is a representative example from our grid of models for each "Self-Pollution Group" (see text for details on the groups). Black lines indicate phases of the evolution in which the surface is strongly polluted with CNO nuclides (from the DCF, DSF or 3DU events). Grey (light blue) lines indicate that the surface still retains the initial metal-poor composition. Evolutionary stages and self-pollution sources are marked, as are the mass and metallicity ranges of each group. Question marks indicate unknown upper boundaries (due to the limited mass range of the current study).

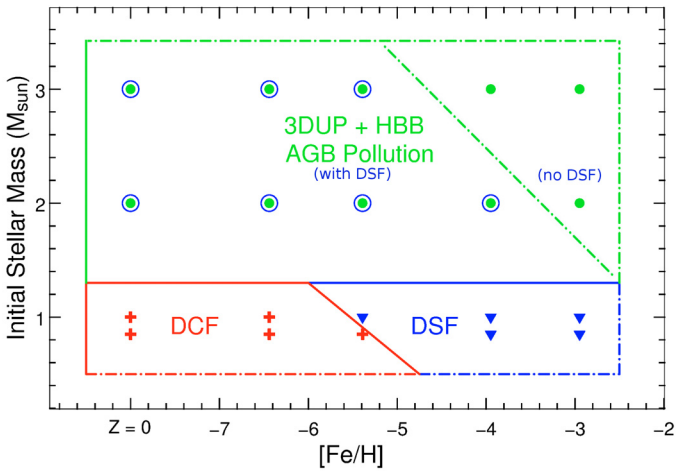

Fig. 4. Mass-metallicity diagram summarising the dominant sources of pollution in the yields. Each symbol represents a single stellar model. Crosses (red) represent the DCF self-pollution Group 1, filled triangles (blue) the DSF Group 2 and filled circles (green) the AGB pollution Group 3. The open circles (blue) around the filled circles (green) indicate intermediate mass models that experienced DSFs. Pollution from TDU (and HBB) easily dominates the pollution from the DSF events at IM mass so the yields of these models fall into the AGB group. The $Z = 0$ models are included at [Fe/H] = −8.

AGB pollution erases the DSF pollution. It can also be seen that the DCF events are limited to ultra metal poor low-mass models, whilst the DSF events occur at higher metallicities (for low mass models). We note that Fujimoto et al. (2000) also provide a mass-metallicity diagram for their low-metallicity study (their Fig. 2). Our diagram is qualitatively similar to theirs. One point of difference is that our boundary for the AGB-DSF models (filled circles with open circles around them in Fig. 4) is at a lower metallicity. This may be due to the fact that we adopt a "hard" Schwarzschild convective boundary in our models, although we are unsure if Fujimoto et al. (2000) used any overshoot or not. A further small difference is that our diagram shows a mass dependence in addition to the metallicity dependency for the pollution event boundaries (diagonal lines in Fig. 4).

3.3. Preliminary comparisons with observations: C and N

In Fig. 5 we compare the carbon yields from our entire grid of models with the observed [C/Fe] abundances in EMP halo stars. It can be seen that the yields are universally C-rich. Thus there is a qualitative agreement between the models and the observations in terms of C, as found by previous studies. Another interesting feature of this diagram is that the model yields predict [C/Fe] to continue increasing towards lower and lower metallicities (stars of such low metallicity may show up in future surveys). Furthermore, taking into account the evolutionary stage at which the surface pollution is gained in the lower mass models (M = 0.85 and 1.0 $M_{\odot}$) – i.e. the DCF events rather than the AGB – the models also predict a higher proportion of C-rich stars at lower and lower metallicities. This is due to the fact that these stars already have self-polluted surfaces during the HB stage – which has a lifetime roughly 1 order of magnitude longer than the AGB phase.

Previous studies have also attempted to quantitatively reproduce the abundances observed in some CEMP stars, in particular C and N. However they have universally found that the 1D models produce by far too much of these elements. The early study

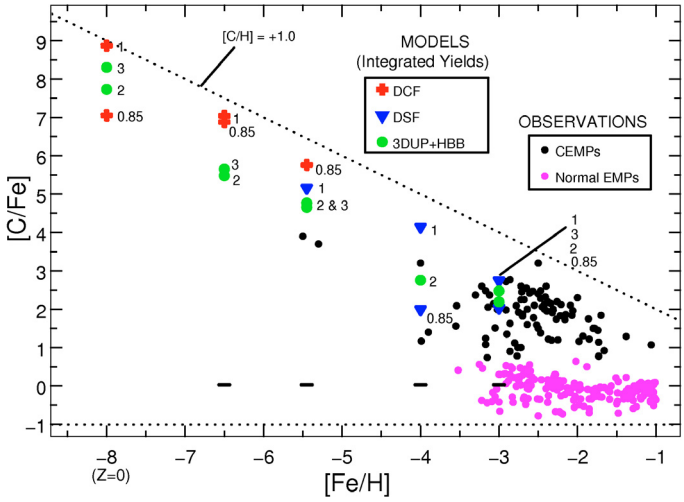

Fig. 5. Carbon yields from our models and observations of EMP stars. Stars with [C/Fe] > +0.7 are shown in black (the CEMPs), those with [C/Fe] < +0.7 are shown in grey (magenta). The short horizontal lines indicate the starting composition of the models (all have [C/Fe] ∼ 0, except for the $Z = 0$ models). We have plotted the $Z = 0$ model yields at [Fe/H] = −8. The two most metal-poor stars can be seen at [Fe/H] ∼ −5.5 (both are C-rich). An upper envelope to the self-pollution of the models – and the observations – is marked by the dotted line at [C/H] = +1.0. The yields from our models are colour- and shape-coded to highlight the different episodes that produced the bulk of the pollution in each yield (see text for details). Numbers beside each yield marker indicate initial stellar mass, in $M_\odot$. The 3 $M_\odot$ model at this [Fe/H] = −4.0 is missing due to a data loss. Observational data are from Frebel et al. (2006); Spite et al. (2006); Aoki et al. (2007); Beers et al. (2007); Cohen et al. (2006); Christlieb et al. (2004) and Aoki et al. (2006b).

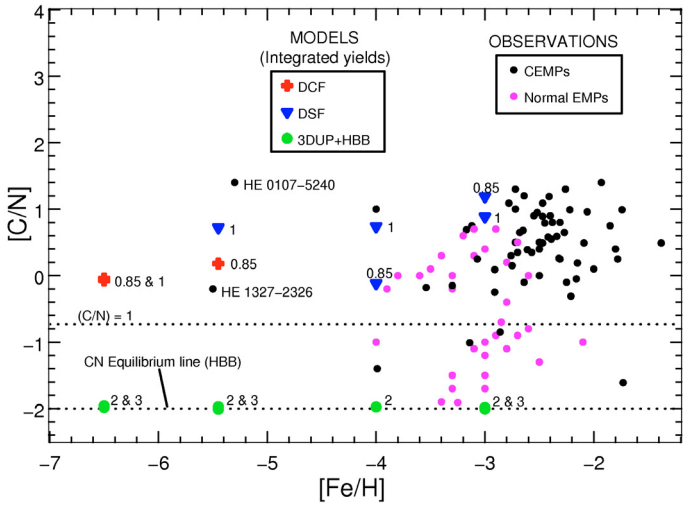

Fig. 6. Comparing the [C/N] ratios in the yields of our models with those of the observations. See Fig. 5 for the observational data sources and the definitions of CEMPs and "normal" EMPs. We have marked in the CN equilibrium line (for HBB) at [C/N] = −2 (i.e. C/N = 0.05). All the models that experienced HBB fall on this line. We have also marked in a dotted line at [C/N] ∼ −0.8 which is where C/N ∼ 1, so that C dominates N above this line. For reference [C/N] = +1 is equivalent to C/N ∼ 50. Note that we have not plotted the $Z = 0$ models in this case.

by Hollowell et al. (1990) reported their resultant post-DCF surface abundance of nitrogen to be ∼10^2 times that observed in the EMP star CD−38 245. Schlattl et al. (2002) find about the same two orders of magnitude overproduction of both N and C, whilst Iwamoto et al. (2004) find their [Fe/H] = −2.7 models produce ∼1 to 2 dex too much C and N than observed.

In Fig. 5 it can be seen that our models produce similar overabundances at the lowest metallicities. For instance, at [Fe/H] = −5.5, the current lower limit of the observations, our models produce ∼1 to 2 dex too much C. Our findings thus concur with the previous studies – the DCF self-pollution scenario is not viable for these stars (also see Picardi et al. 2004), at least in terms of current 1D models. We note however that the overabundance problem may be alleviated somewhat in a binary mass-transfer scenario whereby the material would be diluted in the secondary star's envelope. Interestingly at this metallicity it is the higher mass models (2 and 3 $M_\odot$), which have yields dominated by AGB products, that are the closest to the observations – their yields are only ∼0.7 dex overabundant in C. However these models have undergone strong HBB (see Fig. 2), which has made their yields highly N-rich and thus pushed their [C/N] ratios well below the CEMP observations (Fig. 6).

At [Fe/H] = −4.0 our yields are more consistent with the observations, although the 1 $M_\odot$ model still produces ∼1 dex too much C. It is important to note here that the observational data samples at these ultra low metallicities are still very small (e.g. there are only two stars at [Fe/H] ∼ −5.5).

At [Fe/H] = −3.0 the data sample is much larger. Here we find that our carbon results are much more in line with observations. At this metallicity DCFs are not found to occur (see Figs. 3 and 4). Instead the lower mass models experience Dual *Shell* Flashes at the start of the AGB. Since they do not show TDU the abundance patterns in their yields are primarily from the DSFs. The higher mass models do not undergo any Dual Flashes at all, they experience normal AGB TDU and strong HBB (even at 2 $M_\odot$). However the low [C/N] ratios in the yields from these IM models are again too low compared to the observations. Thus, based on the two constraints of [C/Fe] and [C/N], it is our low mass models which undergo DSFs that provide the best fit to the observations. We note that our results are in contrast with the models of Iwamoto et al. (2004), who found their [Fe/H] = −2.7 models to produce ∼1 to 2 dex too much C and N.

We display some [C/N] ratios from EMP Galactic Halo star observations along with our yield abundances in Fig. 6. An interesting feature of the observations is that the bulk of the CEMPs have [C/N] values ranging from Solar to ∼1 dex super-solar (which corresponds to C/N ∼ 50). In contrast the "normal" (non C-rich) EMPs show a very large spread, from 2 dex sub-solar to 1 dex super-solar. An important point here is that the CEMPs are simultaneously C- and N-rich – although they generally have lower N abundances than C, they are also strongly enriched in N. The newly constructed "Stellar Abundances for Galactic Archeology" (SAGA) Internet database of Suda et al. (2008), which contains more observational data, also shows these features.

The "dual pollution" of C and N is qualitatively similar to the pollution found to arise from the Dual Flashes, a result that has been reported by a number of previous studies (e.g. Hollowell et al. 1990; Schlattl et al. 2002). Significantly this contrasts with the chemical pollution expected from TDU in low mass stars, which would be predominately C-rich. As mentioned above, the yields from the models which suffer HBB are heavily enriched in N – so much so that N rather than C dominates their composition – in contrast to the DF-polluted yields. Thus the yields from intermediate mass AGB stars can not reproduce the bulk of the CEMP observations (we note that there are a few CEMPs located below the C/N = 1 line; also see Johnson et al. 2007 for an analysis of the apparent paucity of N-rich CEMPs).

In Fig. 6 it can also be seen that the spread of [C/N] values in the yields dominated by the DF events (i.e. the low-mass models) are reasonably consistent with the spread of the CEMP observations. Again at the lowest metallicities ([Fe/H] = −5.5, −4.0) we are dealing with very small samples (2 or 3 stars). The main discrepancy is HE 0107−5240 which has a [C/N] ratio significantly above that of our models of comparable metallicity. We note that Venn & Lambert (2008) have recently suggested that some of the most metal-deficient Halo stars, such as this one, may actually be low-metallicity analogues of the "chemically peculiar" stars (which show dust depletion of particular elements, such as Fe) and thus may be intrinsically more metal-rich than currently thought.

The yields from our higher metallicity low-mass models ([Fe/H] = −3.0) are at the high end of the observations ([C/N] ∼ 1). Looking back at Fig. 5 the reason for this seems to be that our models produce C at the upper end of the CEMP distribution. One possible solution to this is dilution of the C-rich material with scaled-solar C/Fe in a binary mass-transfer scenario. Another possibility is that the Dual Shell Flash events – which we stress are the only events that come close to simultaneously reproducing the [C/Fe] and [C/N] observations – may in reality produce a distribution of C (and N) pollution that is not reflected in the models.

It is interesting to note that other objects also show surfaces simultaneously enriched in C and N. Recent observations of potential "Late Hot Flasher" stars (see Sect. 3.1) show this feature (e.g. Lanz et al. 2004), as does Sakurai's Object, one of the few known "Born-Again" AGB stars (Asplund et al. 1999). The fact that the chemical patterns in these two types of objects are thought to arise from He-flash induced H-ingestion episodes lends weight to the suggestion that the CEMP abundance patterns are a product of the similar phenomenon of EMP Dual Flashes.

Although the Dual Flash [C/Fe] and [C/N] abundances in the yields compare reasonably with the observations, the lifetimes of these stars also need to be taken into account. We find models with initial masses of 0.85 $M_{\odot}$ (i.e. the low-mass edge of our grid) have lifetimes of ∼10 Gyr. This is comparable to the age of the Galactic Halo Globular clusters so these stars may still be "living" today. Conversely the 1, 2 and 3 $M_{\odot}$ models, which have main sequence lifetimes of ∼5.7, ∼0.6 and ∼0.2 Gyr respectively, would not have lasted to the present day. They could however have contributed to the chemical enrichment of the CEMP population through binary mass transfers (see e.g. Suda et al. 2004; Lucatello et al. 2005; Stancliffe et al. 2007; Lugaro et al. 2008).

Finally we note that here we have only discussed the chemical signatures of C and N. We shall provide further comparisons and analysis of other elements and abundance patterns in future papers in this series.

3.4. Uncertainties and the way forward

The results presented here naturally contain many uncertainties, especially since they are the first attempt at detailed yields in this mass and metallicity range, and particularly because EMP stellar evolution is so challenging.

Some sources of uncertainties include: the unknown mass-loss rates, uncertain nuclear reaction rates and the treatment of convection and mixing. Testing all of these uncertainties is outside the scope of this study, and indeed would require an extremely large amount of work (it is somewhat more tractable using synthetic stellar models, see e.g. Marigo 2001).

Determining some bounds to AGB model results has however been attempted by various studies. For instance our group explored the effects of varying mass-loss rates and (some) nuclear reaction rates in low and intermediate mass stars of low metallicity (Fenner et al. 2004). A more detailed study into the mass-loss dependence of AGB yields was recently reported by Stancliffe & Jeffery (2007), and Herwig et al. (2006) investigated the effect of reaction rate uncertainties on TDU efficiency and the resultant AGB yields. A further source of uncertainty arises because detailed AGB models are currently lacking opacity tables that take into account the C and N enrichment that occurs as a result of 3DU and HBB. In particular low temperature opacity tables variable in H, He, C and N (at least) are needed. By approximating the opacity of a few key molecules in synthetic stellar models, Marigo (2002) showed how important including this opacity source is. She found, amongst other things, that it affects the effective temperature and lifetime of C-rich models. We note that Lederer & Aringer (2008) have just completed detailed calculations to produce tables for use in AGB stellar models. Some preliminary results have recently been used in a study by Cristallo et al. (2007). We are currently updating our structure code to include these opacity tables.

In the case of the $Z = 0$ and EMP models considered here another source of uncertainty arises – that of handling the violent Dual Flash events. Schlattl et al. (2001) investigated the dependence of the H-ingestion flashes on physical inputs, finding that the occurrence of DFs is dependent on, for example, the initial He abundance and the inclusion of atomic diffusion. They did however conclude that DFs are a robust prediction of 1D stellar models. They also noted that the degree and type of pollution arising from their models is very similar to previous studies. It is reassuring that all 1D DCF simulations appear to give very similar results, despite the various numerical methods employed between codes. However, seeing as most of the models overestimate the amount of C and N production by orders of magnitude (see Sect. 3.3), this general agreement may just reflect a consistent inadequacy of the 1D codes in handling the DCF events. For this reason we believe that multidimensional fluid dynamics calculations are really needed to model these violent episodes. This area of research is in its infancy, however a couple of groups (e.g. our group and Woodward et al. 2008) have recently attempted preliminary simulations. As the fluid dynamics calculations are limited to very short timescales – a simulation of a few hours of star-time takes ∼1 month on 32 processors (private communication, Mocak 2008) – the results from this work will still need to be parameterised for use in 1D stellar codes. The fluid dynamics simulations will eventually give important information on the mixing velocities and the behaviour of convective boundaries in this extreme environment, hopefully shedding light on the reason for the overproduction of C and N in the 1D models.

4. Summary

We have modified an existing stellar code and used this to calculate the evolution and nucleosynthesis of a grid of low- and intermediate-mass EMP and $Z = 0$ models, from the ZAMS to the end of the TPAGB. In this paper, the first of a series to analyse the large amount of data produced, we have presented the yields for the 20 stars. We also briefly analysed the C and N yields in the context of the Galactic Halo CEMP population.

We find that the yields are universally C-rich, in qualitative agreement with the CEMP observations. However, as previous studies have found, our yields do not fit quantitatively – most of the C yields are too high to explain the most metal-poor objects

([Fe/H] $\lesssim -4.0$). The disagreement is at the ∼1 to 2 dex level, as also found previous studies. Dilution of the yields through binary mass transfer or better numerical modelling may resolve this discrepancy. We also note that the very small observational data sets at these extreme metallicities make comparisons uncertain.

At higher metallicities ([Fe/H] ~ -3.0), where the observational data set is much larger, we find that the C yields of our [Fe/H] = −3.0 models are compatible with the most C-rich CEMPs. Importantly it is the models that have their yields dominated by the Dual Shell Flash pollution (our "Group 2" yields) that best match the observations, based on the two constraints considered here – [C/Fe] and [C/N]. The models that have their yields dominated by TDU and HBB produce comparable amounts of C but have too much N (generated from the HBB), which pushes [C/N] to much lower values than seen in the observations. Moreover, if the lower mass stars were to experience TDU (and no DFs), the pollution expected would be (mainly) C-rich, whereas the CEMPs are enriched in N as well as C. Thus TDU – with or without HBB – does not seem to be a viable solution for the CEMP abundance patterns. We stress that the Dual Shell Flash events only occur at low metallicities. We note that our result is in contrast with the findings of Iwamoto et al. (2004) who found their [Fe/H] = −2.7 models to produce ∼1 to 2 dex too much C relative to the observations.

We also find that the models predict [C/Fe] to increase at lower and lower metallicities. Furthermore, the proportion of CEMP stars should also continue to increase at lower metallicities, based on the results that some of the low mass EMP models already have polluted surfaces by the HB phase (which has a long lifetime compared to the AGB), and that there are more C-producing evolutionary episodes at these metallicities.

Finally we note that all of these calculations contain many uncertainties. These include the unknown mass-loss rates, uncertain nuclear reaction rates, the treatment of convection and opacities. In the case of the Dual Flash events we believe this warrants multidimensional fluid dynamics calculations, which a number of groups have started working on.

The models and yields from this study will be described in more detail in future papers in this series.

Acknowledgements. This study utilised the Australian Partnership for Advanced Computing (APAC) supercomputer, under Project Code *g61*. SWC thanks the original authors and maintainers of the stellar codes that have been used in this work – Peter Wood, Rob Cannon, John Lattanzio, Maria Lugaro, Amanda Karakas, Cheryl Frost, Don Faulkner and Bob Gingold. SWC was supported by a Monash University Research Graduate School Ph.D. scholarship for 3.5 years.

References

Aoki, W., Bisterzo, S., Gallino, R., et al. 2006a, ApJ, 650, L127
Aoki, W., Frebel, A., Christlieb, N., et al. 2006b, ApJ, 639, 897
Aoki, W., Beers, T. C., Christlieb, N., et al. 2007, ApJ, 655, 492
Asplund, M., Gustafsson, B., Lambert, D. L., & Kameswara Rao, N. 1997, A&A, 321, L17
Asplund, M., Lambert, D. L., Kipper, T., Pollacco, D., & Shetrone, M. D. 1999, A&A, 343, 507
Beers, T., & Christlieb, N. 2005, ARA&A, 43, 531
Beers, T. C., Sivarani, T., Marsteller, B., et al. 2007, AJ, 133, 1193
Brown, T. M., Sweigart, A. V., Lanz, T., Landsman, W. B., & Hubeny, I. 2001, ApJ, 562, 368
Cannon, R. C. 1993, MNRAS, 263, 817
Cassisi, S., & Castellani, V. 1993, ApJS, 88, 509
Cassisi, S., Castellani, V., & Tornambe, A. 1996, ApJ, 459, 298
Cassisi, S., Schlattl, H., Salaris, M., & Weiss, A. 2003, ApJ, 582, L43
Chieffi, A., Domínguez, I., Limongi, M., & Straniero, O. 2001, ApJ, 554, 1159
Christlieb, N., Gustafsson, B., Korn, A. J., et al. 2004, ApJ, 603, 708
Coc, A., Vangioni-Flam, E., Descouvemont, P., Adahchour, A., & Angulo, C. 2004, ApJ, 600, 544
Cohen, J. G., Shectman, S., Thompson, I., et al. 2005, ApJ, 633, L109
Cohen, J. G., McWilliam, A., Shectman, S., et al. 2006, AJ, 132, 137
Cristallo, S., Straniero, O., Lederer, M. T., & Aringer, B. 2007, ApJ, 667, 489
D'Antona, F. 1982, A&A, 115, L1
Ezer, D. 1961, ApJ, 133, 159
Fenner, Y., Campbell, S., Karakas, A. I., Lattanzio, J. C., & Gibson, B. K. 2004, MNRAS, 353, 789
Ferguson, J. W., Alexander, D. R., Allard, F., et al. 2005, ApJ, 623, 585
Frebel, A., Aoki, W., Christlieb, N., et al. 2005, Nature, 434, 871
Frebel, A., Christlieb, N., Norris, J. E., et al. 2006, ApJ, 652, 1585
Frost, C. A., & Lattanzio, J. C. 1996, ApJ, 473, 383
Fujimoto, M. Y., Iben, I. J., & Hollowell, D. 1990, ApJ, 349, 580
Fujimoto, M. Y., Ikeda, Y., & Iben, I. J. 2000, ApJ, 529, L25
Goriely, S., & Siess, L. 2001, A&A, 378, L25
Goswami, A., Aoki, W., Beers, T. C., et al. 2006, MNRAS, 372, 343
Herwig, F., Blöcker, T., Langer, N., & Driebe, T. 1999, A&A, 349, L5
Herwig, F., Austin, S. M., & Lattanzio, J. C. 2006, Phys. Rev. C, 73, 025802
Hollowell, D., Iben, I. J., & Fujimoto, M. Y. 1990, ApJ, 351, 245
Iben, Jr., I., Kaler, J. B., Truran, J. W., & Renzini, A. 1983, ApJ, 264, 605
Iglesias, C. A., & Rogers, F. J. 1996, ApJ, 464, 943
Iwamoto, N., Kajino, T., Mathews, G. J., Fujimoto, M. Y., & Aoki, W. 2004, ApJ, 602, 377
Johnson, J. A., Herwig, F., Beers, T. C., & Christlieb, N. 2007, ApJ, 658, 1203
Karakas, A. I. 2003, Ph.D. Thesis (Australia: Monash University)
Lanz, T., Brown, T. M., Sweigart, A. V., Hubeny, I., & Landsman, W. B. 2004, ApJ, 602, 342
Lattanzio, J., Frost, C., Cannon, R., & Wood, P. R. 1996, MmSAI, 67, 729
Lederer, M. T., & Aringer, B. 2008, A&A, submitted
Limongi, M., Chieffi, A., & Bonifacio, P. 2003, ApJ, 594, L123
Lucatello, S., Tsangarides, S., Beers, T. C., et al. 2005, ApJ, 625, 825
Lucatello, S., Beers, T. C., Christlieb, N., et al. 2006, ApJ, 652, L37
Lugaro, M., Ugalde, C., Karakas, A. I., et al. 2004, ApJ, 615, 934
Lugaro, M., de Mink, S. E., Izzard, R. G., et al. 2008, A&A, 484, L27
Marigo, P. 2001, A&A, 370, 194
Marigo, P. 2002, A&A, 387, 507
Marigo, P., Girardi, L., Chiosi, C., & Wood, P. R. 2001, A&A, 371, 152
Meynet, G., Maeder, A., & Mowlavi, N. 2004, A&A, 416, 1023
Picardi, I., Chieffi, A., Limongi, M., et al. 2004, ApJ, 609, 1035
Reimers, D. 1975, Mem. Soc. Roy. Sci. Liège, 8, 369
Renzini, A. 1990, ASPC, 11, 549
Schlattl, H., Cassisi, S., Salaris, M., & Weiss, A. 2001, ApJ, 559, 1082
Schlattl, H., Salaris, M., Cassisi, S., & Weiss, A. 2002, A&A, 395, 77
Shigeyama, T., & Tsujimoto, T. 1998, ApJ, 507, L135
Siess, L., Livio, M., & Lattanzio, J. 2002, ApJ, 570, 329
Sivarani, T., Beers, T. C., Bonifacio, P., et al. 2006, A&A, 459, 125
Spite, M., Cayrel, R., Hill, V., et al. 2006, A&A, 455, 291
Stancliffe, R. J. 2006, MNRAS, 370, 1817
Stancliffe, R. J., & Jeffery, C. S. 2007, MNRAS, 375, 1280
Stancliffe, R. J., Glebbeek, E., Izzard, R. G., & Pols, O. R. 2007, ArXiv Astrophysics e-prints
Suda, T., Aikawa, M., Machida, M. N., Fujimoto, M. Y., & Iben, I. J. 2004, ApJ, 611, 476
Suda, T., Katsuta, Y., Yamada, S., et al. 2008, PASJ, 60, in press
Sweigart, A. V. 1997, in The Third Conference on Faint Blue Stars, ed. A. G. D. Philip, J. Liebert, R. Saffer, & D. S. Hayes, 3
Vassiliadis, E., & Wood, P. R. 1993, ApJ, 413, 641
Venn, K. A., & Lambert, D. L. 2008, ApJ, 677, 572
Weiss, A., Schlattl, H., Salaris, M., & Cassisi, S. 2004, A&A, 422, 217
Wood, P. R., & Zarro, D. M. 1981, ApJ, 247, 247
Woodward, P., Herwig, F., Porter, D., et al. 2008, First Stars III: First Stars II Conference, AIP Conf. Proc., 990, 300